Electronic Supporting Information

Time-resolved infra-red studies of photo-excited porphyrins in the presence of nucleic acids and in HeLa tumour cells: insights into binding site and electron transfer dynamics

Páraic M. Keane,[ab]* Clara Zehe,[c] Fergus E. Poynton,[ad] Sandra A. Bright,[ad] Sandra Estayalo-Adrián, [ad] Stephen J. Devereux,[c] Paul M. Donaldson,[e] Igor V. Sazanovich,[e] Michael Towrie,[e] Stanley W. Botchway,[e] Christine J. Cardin,[b] D. Clive Williams,[d] Thorfinnur Gunnlaugsson,[ad] Conor Long,[f]* John M. Kelly,[a]* Susan J. Quinn[c]*

[a]*School of Chemistry, Trinity College Dublin, Dublin 2, Ireland.*
email: keanepa@tcd.ie; jmkelly@tcd.ie
[b]*School of Chemistry, University of Reading. Whiteknights, Reading RG6 6AD, U.K.*
[c]*School of Chemistry, University College Dublin, Dublin 4, Ireland*
email: susan.quinn@ucd.ie
[d]*Trinity Biomedical Sciences Institute, The University of Dublin, Pearse St., Dublin 2, Ireland*
[e]*STFC Central Laser Facility, Research Complex at Harwell, Rutherford Appleton Laboratory, Didcot OX11 0QX, U.K.*
[f]*School of Chemical Sciences, Dublin City University, Dublin 9, Ireland*
email: conor.long@dcu.ie

Figures

Fig. S1 Ps-TRIR spectra of PtTMPyP4 (500 µM) in phosphate-buffered D_2O and kinetics at 1518 cm^{-1} and 1636 cm^{-1}

Fig. S2 Exponential fits to PtTMPyP4, unbound and in the presence of nucleic acids, at 1620 cm^{-1}

Fig. S3 Ps-TA spectra of PtTMPyP4, PtTMPyP4 + GMP and PtTMPyP4 + $\{d(GC)_5\}_2$ following 400 nm excitation.

Fig. S4 Monoexponential fitting of TMPyP4 at 1638 cm^{-1} and 1513 cm^{-1}

Fig. S5 Comparison of H/D substitution on calculated IR spectra of ground state, singlet excited state and one-electron reduced species.

Fig. S6 Exponential fits to TMPyP4, TMPyP4-GMP, TMPyP4-$\{d(GC)_5\}_2$, TMPyP4-$\{d(CGCAAATTTGCG)\}_2$ and TMPyP4-cMYC unbound and in the presence of nucleic acids, at 1620 cm^{-1}

Fig. S7 Kinetics of transient (1636 cm^{-1}) and bleach (1646 cm^{-1}) for TMPyP4 + GMP, TMPyP4 + $\{d(GC)_5\}_2$ and TMPyP4 + c-MYC quadruplex

Fig. S8 Ps-TA spectra of TMPyP4, TMPyP4-GMP and TMPyP4-$\{d(GC)_5\}_2$

Fig. S9 Biexponential fit of ps-TA of TMPyP4-GMP at 460 nm and 430 nm

Fig. S10 UV/Visible absorption spectra of fixed HeLa cells in the absence of treatment and after treatment with PtTMPyP4 (100 μM) for 4 h

Fig. S11 UV/Visible absorption spectrum PtTMPyP4 (20 μM) in cell culture medium.

Fig. S12 FTIR spectrum of fixed HeLa cells, fixed Hela cells that were treated with PtTMPyP4 (100 μM) for 4 h

Fig. S13 Ps-TRIR spectra of untreated methanol-fixed HeLa cells

Fig. S14 Comparison of calculated $[PtTMPyP4]^{3+}$ reduced state with the calculated ground state (singlet) and triplet state of PtTMPyP4, and calculated difference spectrum obtained for the porphyrin triplet and the reduced state

Tables

Table S1 Exponential fitting parameters

Table S2 The calculated IR absorptions of PtTMPyP4 with intensities greater than 10 (M^{-1} cm^{-1}) in the 1450 to 1700 cm^{-1} region with assignments based on the largest displacement vectors

Table S3 Table of structural parameters for optimised PtTMPyP4 including atom numbering used

Table S4 Coordinates of the optimised ground state of PtTMPyP4 in water

Table S5 Coordinates of the optimised ground state of D_2TMPyP4 in water

Table S6 Coordinates of the optimised first singlet excited state of D_2TMPyP4 in water

Table S7 TRIR kinetic fits – TMPyP4 + GMP/$\{d(GC)_5\}_2$

Table S8 Biexponential fits to ps-TA data of TMPyP4-GMP

Experimental

References

Figures and Tables

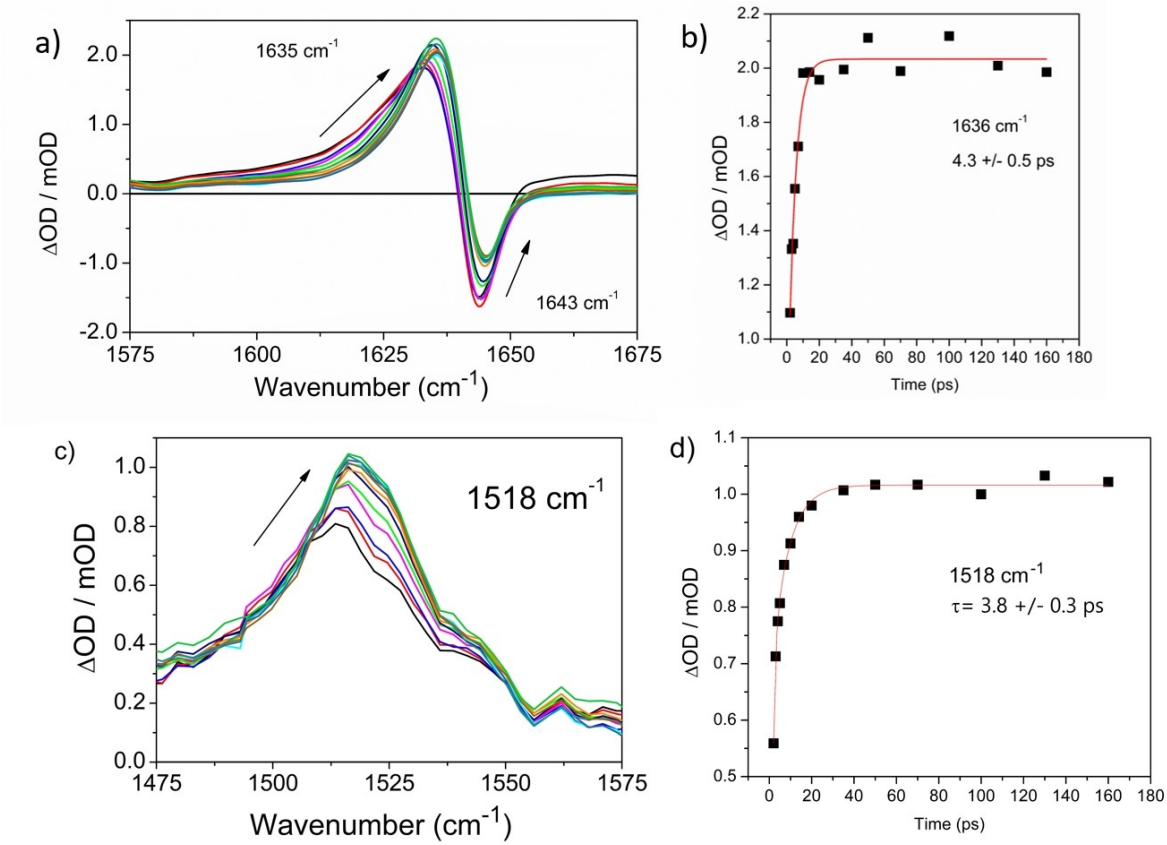

Fig. S1 (a) Ps-TRIR spectra of PtTMPyP4 (500 µM) in phosphate-buffered (50 mM, pH 7) D_2O between 1575 and 1675 cm^{-1} after 400 nm excitation (1 µJ, 10 kHz) at delays between 1 – 200 ps. (b) kinetics at 1636 cm^{-1}, (c) ps-TRIR spectra recorded between 1475 – 1575 cm^{-1} and (d) the kinetics at 1518 cm^{-1}.

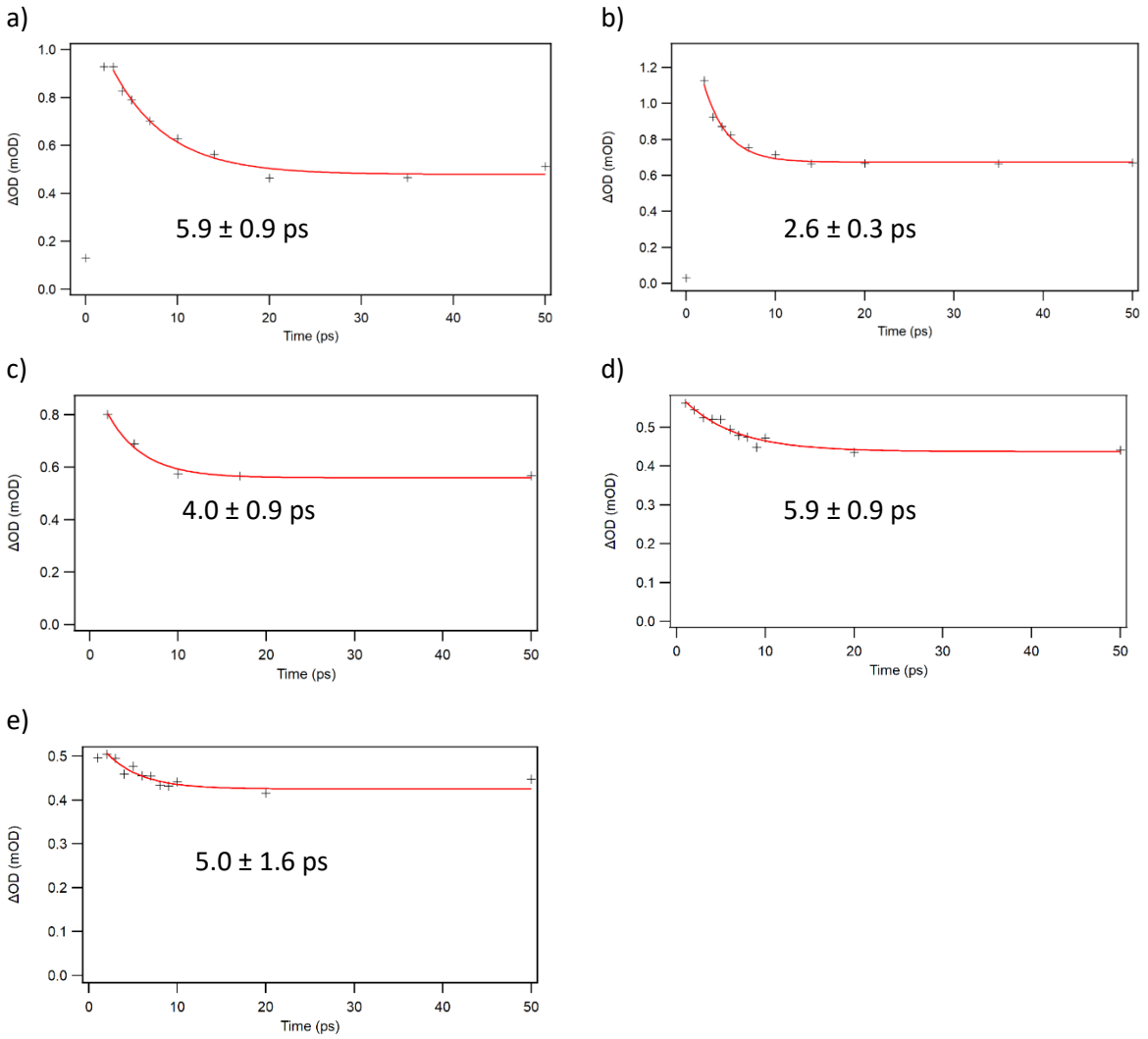

Fig. S2 Exponential fits to PtTMPyP4, unbound and in the presence of nucleic acids, at 1620 cm^{-1} (a) PtTMPyP4, (b) PtTMPyP4-GMP, (c) PtTMPyP4-$\{(GC)_5\}_2$, (d) PtTMPyP4-$\{d(CGCAAATTTGCG)\}_2$, (e) PtTMPyP4-cMYC. Lifetime values shown under plots

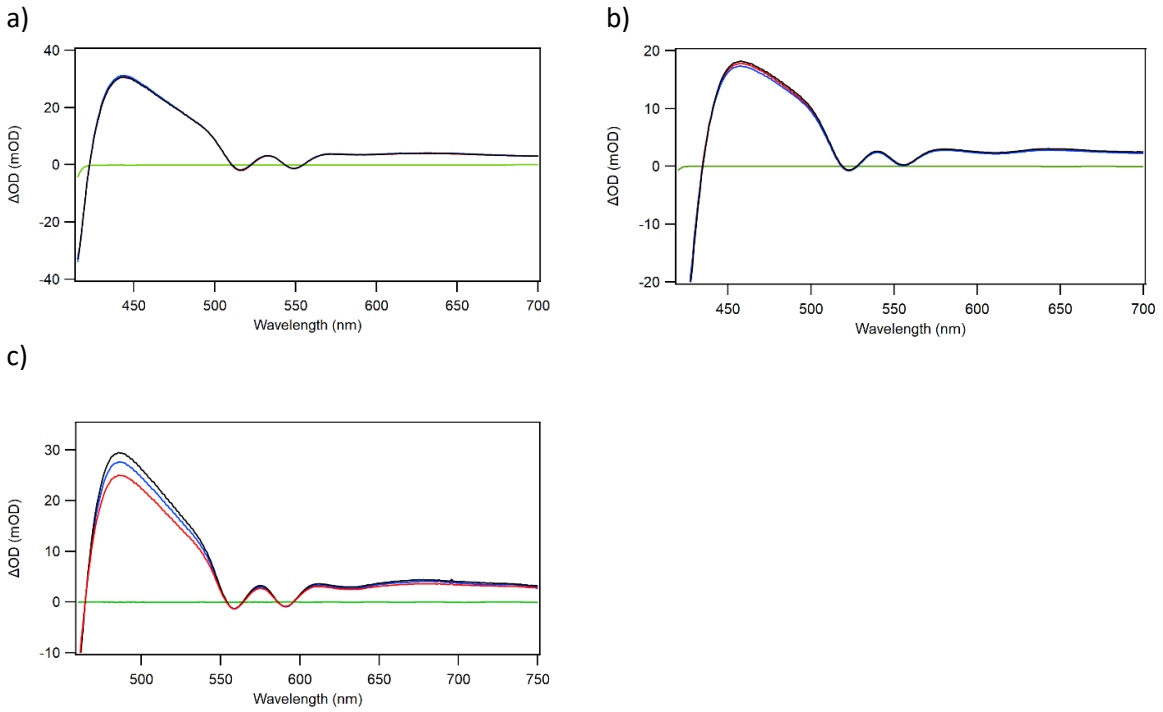

Fig. S3 Ps-TA spectra of (a) PtTMPyP4, (b) PtTMPyP4 + GMP and (c) PtTMPyP4 + $\{d(GC)_5\}_2$ following 400 nm excitation. Delays shown at 3 (red), 10 (blue) and 50 ps (black)

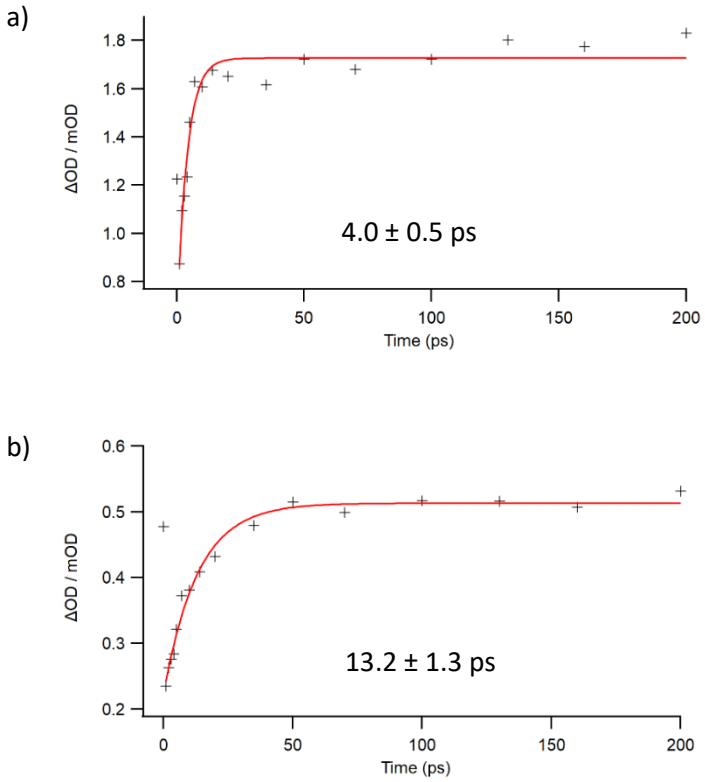

Fig. S4 Monoexponential fitting for TMPyP4 at (a) 1638 cm^{-1} (b) 1513 cm^{-1}. Lifetime values shown under plots

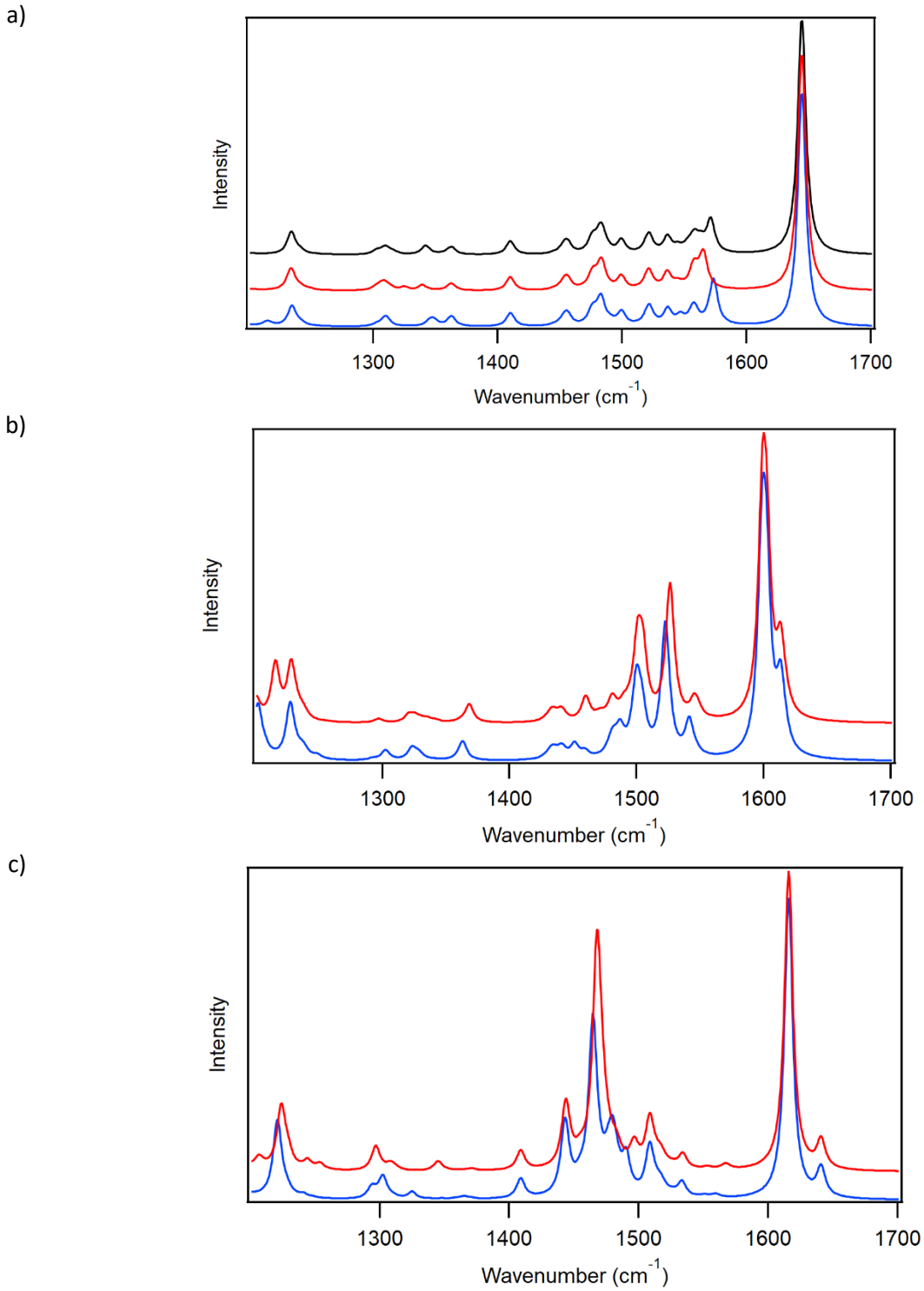

Fig. S5 Comparison of H/D substitution on calculated IR spectra: (a) ground state (b) singlet excited state (c) one-electron reduced species. Red = H_2TMPyP4, Blue = D_2TMPyP4. Black = HDTMPyP4 for (a) only.

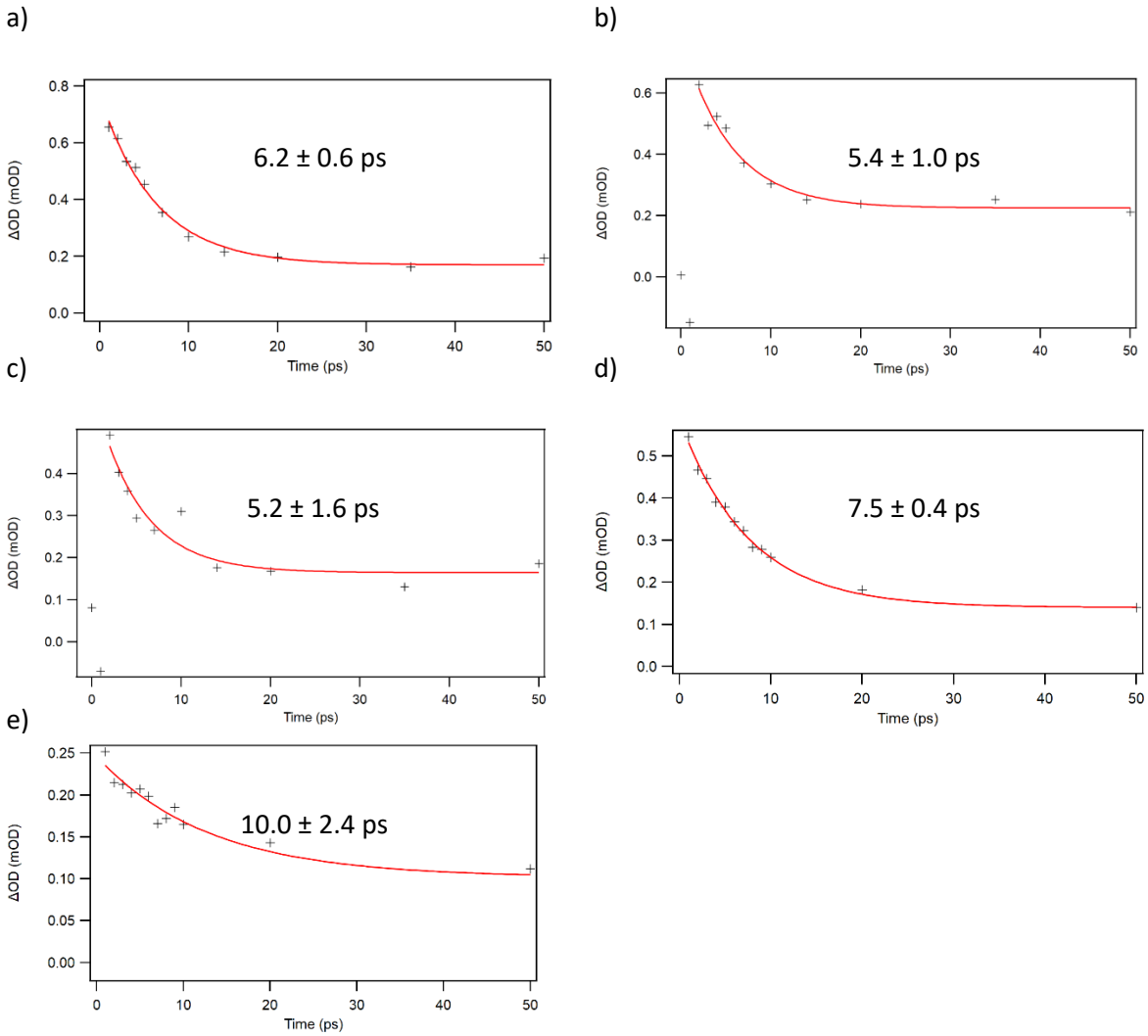

Fig. S6 Exponential fits to (a) TMPyP4, (b) TMPyP4-GMP, (c) TMPyP4-$\{d(GC)_5\}_2$ (d) TMPyP4-$\{d(CGCAAATTTGCG)\}_2$ (e) TMPyP4-cMYC unbound and in presence of nucleic acids, at 1620 cm^{-1}

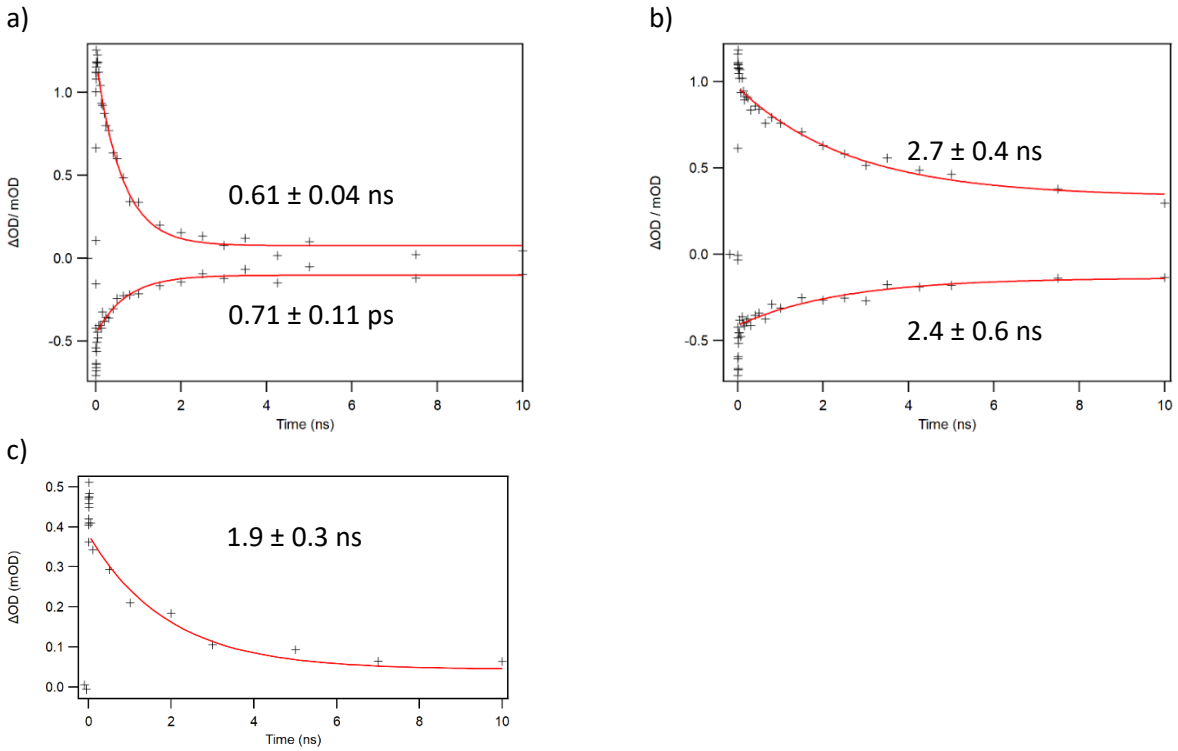

Fig. S7 Kinetics of transient (1636 cm^{-1}) and bleach (where applicable, 1646 cm^{-1}) for (a) TMPyP4 + GMP (b) TMPyP4 + $\{d(GC)_5\}_2$ (c) TMPyP4 + c-MYC quadruplex. Mononexponential fits shown from 50 ps onwards. Fitted lifetime values shown on plots

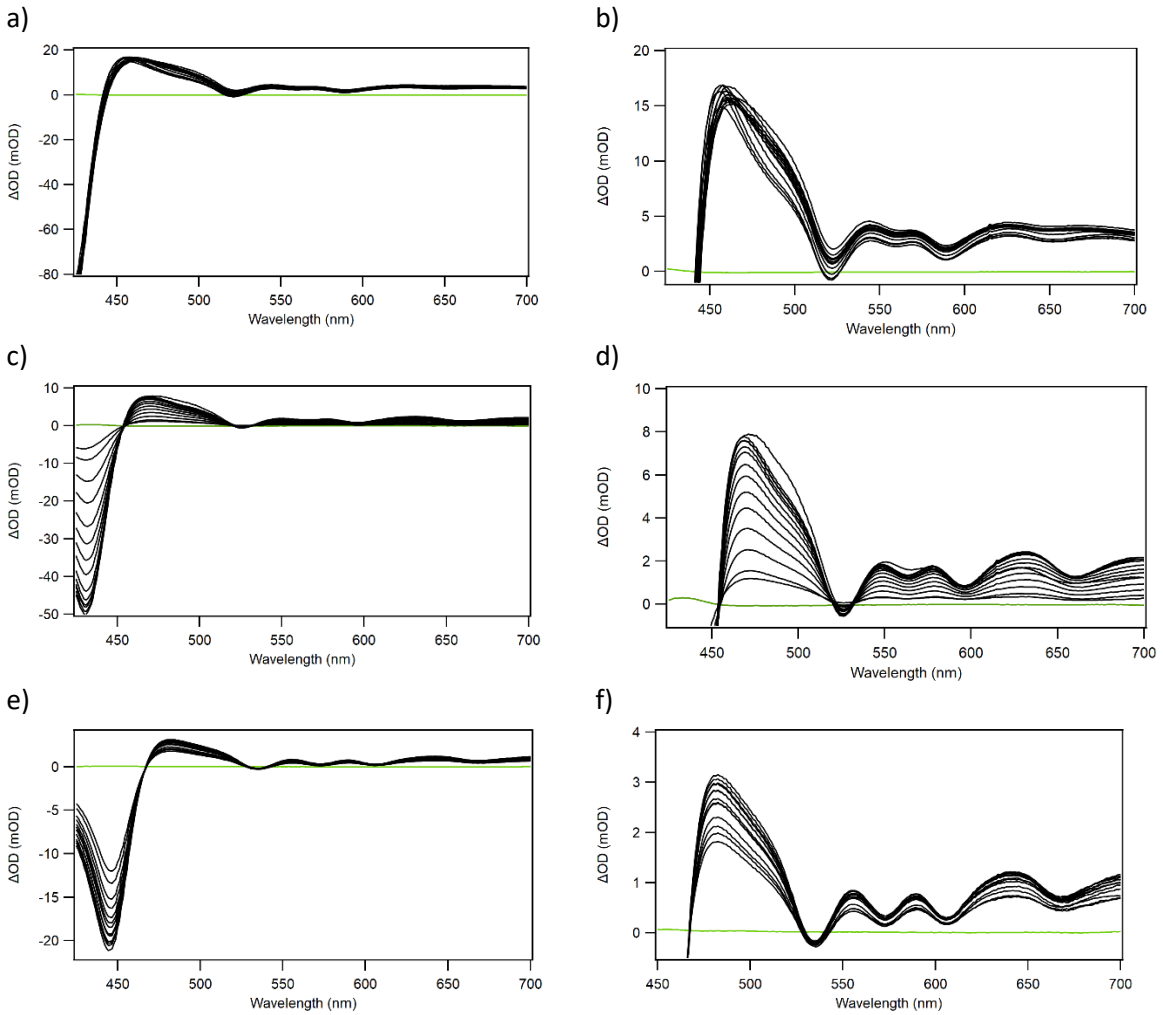

Fig. S8 Ps-TA spectra of (a) TMPyP4 (b) TMPyP4 transient only (c) TMPyP4-GMP (d) TMPyP4-GMP transient only (e) TMPyP4-$\{d(GC)_5\}_2$ (f) TMPyP4-$\{d(GC)_5\}_2$ transient only. 400 nm exc., 1 µJ

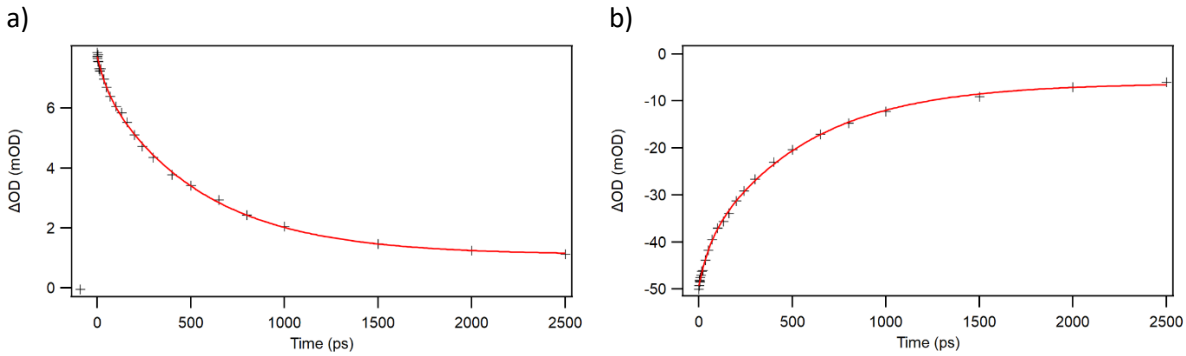

Fig. S9 Biexponential fit of ps-TA of TMPyP4-GMP at (a) 460 nm (b) 430 nm. 400 nm exc.

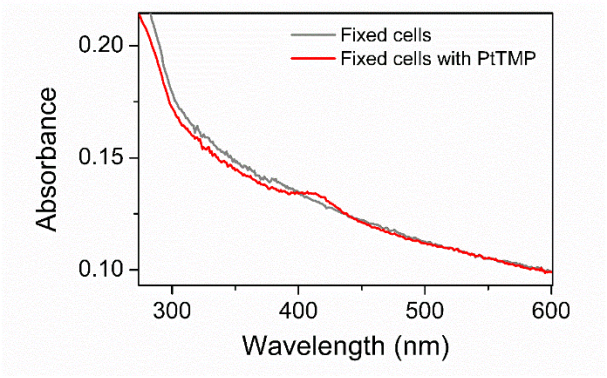

Fig. S10 UV/Visible absorption spectra of fixed HeLa cells in the absence of treatment (grey) and after treatment with PtTMPyP4 (100 µM) for 4 h (red).

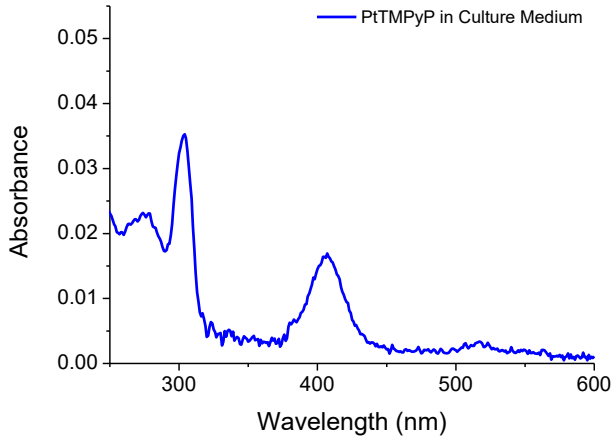

Fig. S11 UV/Visible absorption spectrum of PtTMPyP4 (20 µM) in cell culture medium.

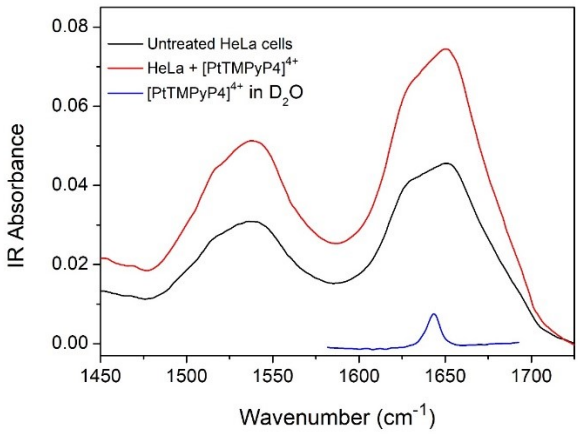

Fig. S12 FTIR spectrum of (a) fixed HeLa cells (b) fixed Hela cells that were treated with PtTMPyP4 (100 µM) for 4 h and (c) PtTMPyP4 (800 µM) in D_2O.

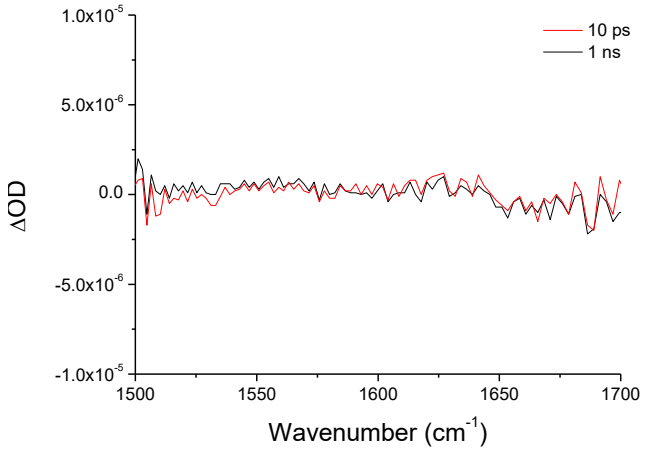

Fig. S13 Ps-TRIR spectra of untreated methanol-fixed HeLa cells after 400 nm excitation (200 nJ, 50 kHz) at 10 ps and 1 ns time delays.

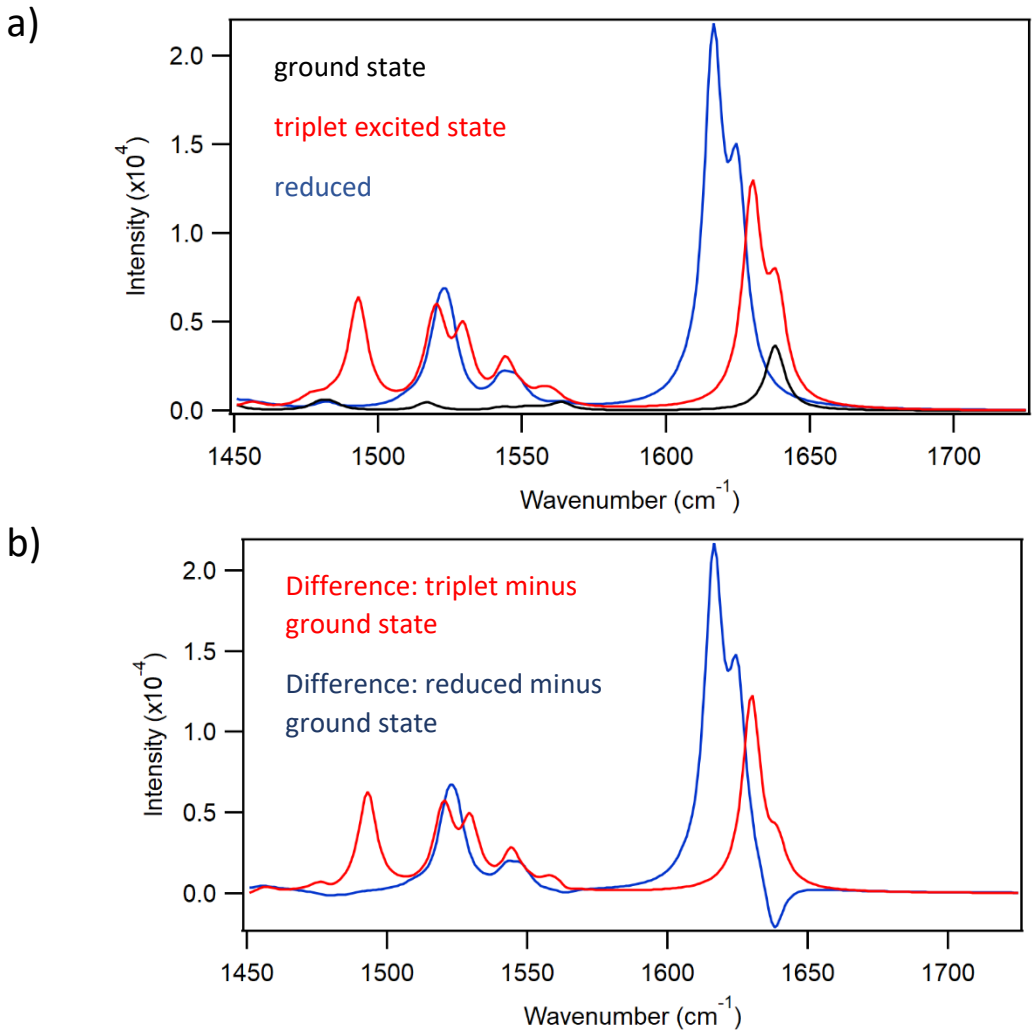

Fig. S14 (a) Comparison of calculated $[PtTMPyP4]^{3+}$ reduced state with the calculated ground state (singlet) and triplet state of PtTMPyP4. (b) calculated difference spectrum obtained for the porphyrin triplet and the reduced state

Table S1 Exponential fitting parameters for presumed vibrational cooling.

system	**wavenumber (cm^{-1})**	**τ (ps)**
PtTMPyP4	1636	4.3 ± 0.5
PtTMPyP4	1518	3.8 ± 0.3
PtTMPyP4	1620	5.9 ± 0.9
PtTMPyP4-GMP	1620	2.6 ± 0.3
PtTMPyP4-$\{d(GC)_5\}_2$	1620	4.0 ± 0.9
PtTMPyP4-$\{d(CGCAAATTTGCG)\}_2$	1620	5.9 ± 0.9
PtTMPyP4-cMYC	1620	5.0 ± 1.6
TMPyP4	1638	4.0 ± 0.5
TMPyP4	1513	13.2 ± 1.3
TMPyP4	1620	6.2 ± 0.6
TMPyP4-GMP	1620	5.4 ± 1.0
TMPyP4-$\{d(GC)_5\}_2$	1620	5.2 ± 1.6
TMPyP4-$\{d(CGCAAATTTGCG)\}_2$	1620	7.5 ± 0.4
TMPyP4-cMYC	1620	10.0 ± 2.4

Table S2 The calculated IR PtTMPyP4 absorptions with intensities greater than 10 (M^{-1} cm^{-1}) in the 1450 to 1700 cm^{-1} region with assignments based on the largest displacement vectors

	Wavenumber				
Mode Number	Unscaled	Scaled (factor 0.9803)	Intensity	Description	
187	1474.81	1445.75	10.7851	N-Me wag	
188	1474.82	1445.77	10.5045	N-Me wag	
190	1479.26	1450.11	30.9619	Pyridinium breathing	
193	1479.53	1450.39	33.148	Pyridinium breathing	
198	1509.17	1479.44	37.2551	N-Me rock	
199	1509.18	1479.45	55.3931	N-Me rock	
200	1509.24	1479.5	18.7789	N-Me rock	
201	1512.95	1483.15	46.8093	N-Me rock	
203	1513.72	1483.9	48.3441	N-Me rock	
204	1514.47	1484.64	14.6004	N-Me rock	
206	1547.33	1516.85	65.7881	Pyridinium breathing	
207	1547.35	1516.87	69.1859	Pyridinium breathing	
212	1574.16	1543.15	19.1395	Pyridinium-Porphyrin breathing	
213	1574.48	1543.46	30.4477	Pyridinium-Porphyrin breathing	
214	1582.1	1550.93	31.9652	Pyridinium breathing	
215	1585.68	1554.44	17.5111	Pyridinium-Porphyrin breathing	
216	1585.76	1554.52	14.5934	Pyridinium-Porphyrin breathing	
217	1589.3	1557.99	10.7115	Pyridinium-Porphyrin breathing	
218	1595.07	1563.65	67.4966	Porphyrin breathing	
219	1595.18	1563.75	67.4399	Porphyrin breathing	
223	1670.81	1637.89	536.5935	Pyridinium breathing	
224	1670.83	1637.92	541.3722	Pyridinium breathing	

Table S3 Table of structural parameters for optimised PtTMPyP4 including atom numbering used

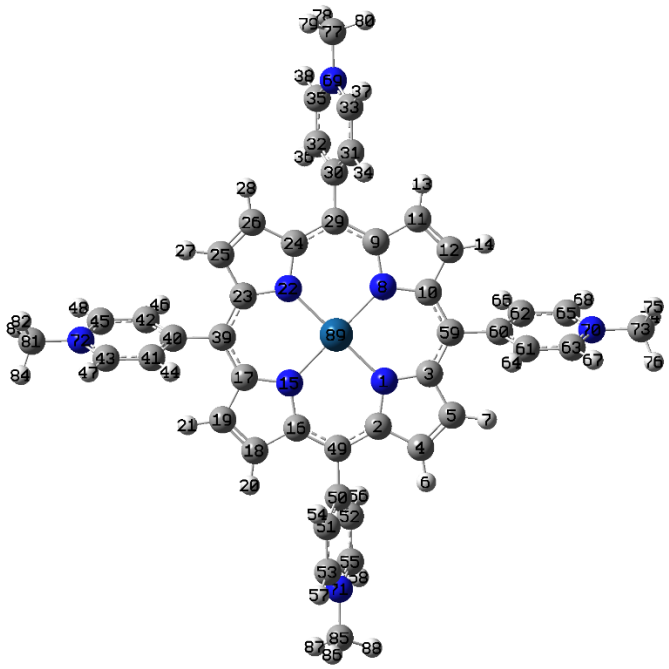

Atom Numbering	
Parameter	Value
R(1,2)	1.3962
R(1,3)	1.3963
R(2,4)	1.4545
R(2,49)	1.4063
R(3,5)	1.4545
R(3,59)	1.4061
R(4,5)	1.368
R(4,6)	1.0794
R(5,7)	1.0794
R(8,9)	1.3962
R(8,10)	1.3964
R(8,89)	2.0458
R(9,11)	1.4545
R(9,29)	1.4063
R(10,12)	1.4545
R(10,59)	1.4061
R(11,12)	1.368
R(11,13)	1.0794
R(12,14)	1.0794
R(15,16)	1.3965
R(15,17)	1.3963

R(15,89)	2.0459
R(16,18)	1.4546
R(16,49)	1.4061
R(17,19)	1.4546
R(17,39)	1.4064
R(18,19)	1.368
R(18,20)	1.0794
R(19,21)	1.0795
R(22,23)	1.3963
R(22,24)	1.3965
R(23,25)	1.4547
R(23,39)	1.4064
R(24,26)	1.4546
R(24,29)	1.4061
R(25,26)	1.368
R(25,27)	1.0794
R(26,28)	1.0795
R(29,30)	1.5037
R(30,31)	1.4168
R(30,32)	1.4147
R(31,33)	1.3951
R(31,34)	1.0844
R(32,35)	1.3975
R(32,36)	1.0844
R(33,37)	1.0842
R(33,69)	1.3692
R(35,38)	1.0836
R(35,69)	1.3671
R(39,40)	1.5033
R(40,41)	1.417
R(40,42)	1.4148
R(41,43)	1.3949
R(41,44)	1.0844
R(42,45)	1.3974
R(42,46)	1.0844
R(43,47)	1.0842
R(43,72)	1.3692
R(45,48)	1.0836
R(45,72)	1.367
R(49,50)	1.5037
R(50,51)	1.4146
R(50,52)	1.4169
R(51,53)	1.3976
R(51,54)	1.0844
R(52,55)	1.395
R(52,56)	1.0844

R(53,57)	1.0836
R(53,71)	1.367
R(55,58)	1.0843
R(55,71)	1.3692
R(59,60)	1.5039
R(60,61)	1.4168
R(60,62)	1.4147
R(61,63)	1.3951
R(61,64)	1.0845
R(62,65)	1.3975
R(62,66)	1.0844
R(63,67)	1.0843
R(63,70)	1.3692
R(65,68)	1.0836
R(65,70)	1.367
R(69,77)	1.5041
R(70,73)	1.5041
R(71,85)	1.5041
R(72,81)	1.5041
R(73,74)	1.091
R(73,75)	1.0936
R(73,76)	1.093
R(77,78)	1.091
R(77,79)	1.0937
R(77,80)	1.0929
R(81,82)	1.0936
R(81,83)	1.091
R(81,84)	1.0931
R(85,86)	1.091
R(85,87)	1.0936
R(85,88)	1.0931
A(2,1,3)	106.6405
A(1,2,4)	109.2453
A(1,2,49)	126.0645
A(4,2,49)	124.6795
A(1,3,5)	109.2443
A(1,3,59)	126.0483
A(5,3,59)	124.6811
A(2,4,5)	107.4344
A(2,4,6)	125.8277
A(5,4,6)	126.7352
A(3,5,4)	107.4329
A(3,5,7)	125.8349
A(4,5,7)	126.7296
A(9,8,10)	106.6403
A(9,8,89)	126.6725

A(10,8,89)	126.6867
A(8,9,11)	109.2463
A(8,9,29)	126.0617
A(11,9,29)	124.6819
A(8,10,12)	109.2411
A(8,10,59)	126.0431
A(12,10,59)	124.6914
A(9,11,12)	107.4356
A(9,11,13)	125.8304
A(12,11,13)	126.7312
A(10,12,11)	107.434
A(10,12,14)	125.8326
A(11,12,14)	126.7312
A(16,15,17)	106.6419
A(16,15,89)	126.6598
A(17,15,89)	126.6703
A(15,16,18)	109.2392
A(15,16,49)	126.0649
A(18,16,49)	124.6726
A(15,17,19)	109.2386
A(15,17,39)	126.0815
A(19,17,39)	124.6545
A(16,18,19)	107.4333
A(16,18,20)	125.8145
A(19,18,20)	126.7319
A(17,19,18)	107.4393
A(17,19,21)	125.8131
A(18,19,21)	126.7242
A(23,22,24)	106.6421
A(22,23,25)	109.2365
A(22,23,39)	126.0684
A(25,23,39)	124.6716
A(22,24,26)	109.2396
A(22,24,29)	126.0727
A(26,24,29)	124.6637
A(23,25,26)	107.4393
A(23,25,27)	125.813
A(26,25,27)	126.7257
A(24,26,25)	107.4348
A(24,26,28)	125.8123
A(25,26,28)	126.7326
A(9,29,24)	124.5158
A(9,29,30)	117.7526
A(24,29,30)	117.7313
A(29,30,31)	121.3096
A(29,30,32)	121.44

A(31,30,32)	117.2503
A(30,31,33)	120.415
A(30,31,34)	120.962
A(33,31,34)	118.6147
A(30,32,35)	120.4541
A(30,32,36)	120.987
A(35,32,36)	118.5488
A(31,33,37)	122.2724
A(31,33,69)	120.8788
A(37,33,69)	116.8477
A(32,35,38)	122.0877
A(32,35,69)	120.8272
A(38,35,69)	117.0843
A(17,39,23)	124.49
A(17,39,40)	117.7425
A(23,39,40)	117.7675
A(39,40,41)	121.3579
A(39,40,42)	121.4176
A(41,40,42)	117.2245
A(40,41,43)	120.426
A(40,41,44)	120.95
A(43,41,44)	118.6147
A(40,42,45)	120.4689
A(40,42,46)	120.9855
A(45,42,46)	118.5345
A(41,43,47)	122.281
A(41,43,72)	120.8864
A(47,43,72)	116.8315
A(42,45,48)	122.0799
A(42,45,72)	120.8282
A(48,45,72)	117.091
A(2,49,16)	124.5135
A(2,49,50)	117.7412
A(16,49,50)	117.7449
A(49,50,51)	121.466
A(49,50,52)	121.283
A(51,50,52)	117.251
A(50,51,53)	120.4537
A(50,51,54)	120.9929
A(53,51,54)	118.5438
A(50,52,55)	120.414
A(50,52,56)	120.9565
A(55,52,56)	118.6208
A(51,53,57)	122.0815
A(51,53,71)	120.8258
A(57,53,71)	117.092

A(52,55,58)	122.2831
A(52,55,71)	120.8796
A(58,55,71)	116.8363
A(3,59,10)	124.5205
A(3,59,60)	117.7348
A(10,59,60)	117.7447
A(59,60,61)	121.3433
A(59,60,62)	121.3895
A(61,60,62)	117.2672
A(60,61,63)	120.4028
A(60,61,64)	120.966
A(63,61,64)	118.6235
A(60,62,65)	120.4468
A(60,62,66)	120.9969
A(65,62,66)	118.547
A(61,63,67)	122.2781
A(61,63,70)	120.8808
A(67,63,70)	116.8401
A(62,65,68)	122.0819
A(62,65,70)	120.8225
A(68,65,70)	117.0948
A(33,69,35)	120.1723
A(33,69,77)	119.2216
A(35,69,77)	120.6028
A(63,70,65)	120.1779
A(63,70,73)	119.1876
A(65,70,73)	120.6328
A(53,71,55)	120.1737
A(53,71,85)	120.659
A(55,71,85)	119.1664
A(43,72,45)	120.1634
A(43,72,81)	119.1828
A(45,72,81)	120.6526
A(70,73,74)	109.4638
A(70,73,75)	109.3592
A(70,73,76)	109.3701
A(74,73,75)	109.4275
A(74,73,76)	109.1832
A(75,73,76)	110.0226
A(69,77,78)	109.46
A(69,77,79)	109.3621
A(69,77,80)	109.3699
A(78,77,79)	109.4749
A(78,77,80)	109.1459
A(79,77,80)	110.0137
A(72,81,82)	109.3591

A(72,81,83)	109.4661
A(72,81,84)	109.3722
A(82,81,83)	109.4079
A(82,81,84)	110.0286
A(83,81,84)	109.1926
A(71,85,86)	109.4685
A(71,85,87)	109.3549
A(71,85,88)	109.3703
A(86,85,87)	109.3939
A(86,85,88)	109.2105
A(87,85,88)	110.0284

Table S4 Coordinates of the optimised ground state of PtTMPyP4 in water

Tag	Symbol	X	Y	Z
1	N	-0.00625	-0.01117	-0.00171
2	C	-0.02231	-0.01058	1.394431
3	C	1.336119	-0.0096	-0.38616
4	C	1.345244	0.000776	1.889613
5	C	2.175056	-0.0052	0.801989
6	H	1.641294	0.020593	2.92747
7	H	3.254377	-0.01487	0.81354
8	N	-0.39192	-0.05492	-2.86838
9	C	-0.77615	-0.05498	-4.21069
10	C	1.004227	-0.07665	-2.85208
11	C	0.411745	-0.08675	-5.04942
12	C	1.499354	-0.09315	-4.21965
13	H	0.422884	-0.11101	-6.12853
14	H	2.537296	-0.10004	-4.51587
15	N	-2.87351	0.024501	0.383877
16	C	-2.489	0.020168	1.726358
17	C	-4.26967	0.023412	0.367803
18	C	-3.67709	-0.00464	2.565134
19	C	-4.76473	-0.0021	1.735358
20	H	-3.68807	-0.04552	3.643753
21	H	-5.80218	-0.0417	2.030912
22	N	-3.25958	-0.04407	-2.48287
23	C	-4.60179	-0.01875	-2.09883
24	C	-3.2431	-0.04583	-3.87923
25	C	-5.43979	0.016089	-3.28737
26	C	-4.60989	-0.00018	-4.37476
27	H	-6.51764	0.07338	-3.29879
28	H	-4.9045	0.041042	-5.41242
29	C	-2.09687	-0.05101	-4.6937
30	C	-2.29742	-0.04746	-6.18399
31	C	-1.95374	1.079802	-6.97046

32	C	-2.83734	-1.16765	-6.85858
33	C	-2.15206	1.064576	-8.35129
34	H	-1.54864	1.976113	-6.51381
35	C	-3.01068	-1.14369	-8.24505
36	H	-3.10771	-2.06795	-6.31799
37	H	-1.91223	1.91473	-8.98001
38	H	-3.40995	-1.99095	-8.78997
39	C	-5.08483	0.008424	-0.77823
40	C	-6.57459	0.022876	-0.57756
41	C	-7.23537	1.155623	-0.04086
42	C	-7.37522	-1.09344	-0.91604
43	C	-8.61937	1.149417	0.133355
44	H	-6.68239	2.049571	0.225615
45	C	-8.75784	-1.06065	-0.71573
46	H	-6.93117	-1.998	-1.3166
47	H	-9.15712	2.004057	0.52831
48	H	-9.39391	-1.9052	-0.95301
49	C	-1.16845	0.003299	2.209164
50	C	-0.96801	-0.00543	3.699449
51	C	-1.29219	1.118665	4.494717
52	C	-0.44695	-1.14256	4.365101
53	C	-1.09355	1.088889	5.877784
54	H	-1.68136	2.026187	4.04656
55	C	-0.27335	-1.13275	5.749194
56	H	-0.1917	-2.04215	3.815922
57	H	-1.32072	1.938899	6.510268
58	H	0.110401	-1.99009	6.290796
59	C	1.81882	-0.04762	-1.70631
60	C	3.309296	-0.05773	-1.90652
61	C	4.100506	1.07934	-1.6094
62	C	3.978867	-1.20253	-2.39886
63	C	5.481336	1.049577	-1.80604
64	H	3.647717	1.99353	-1.24157
65	C	5.3655	-1.19187	-2.57272
66	H	3.434305	-2.11082	-2.63214
67	H	6.114042	1.905789	-1.60063
68	H	5.906595	-2.05734	-2.93657
69	N	-2.67221	-0.03807	-8.97437
70	N	6.099572	-0.07642	-2.27999
71	N	-0.59261	-0.02614	6.489659
72	N	-9.3648	0.050256	-0.19974
73	C	7.58987	-0.0646	-2.48316
74	H	7.926935	-1.06454	-2.76023
75	H	7.841244	0.638433	-3.28228
76	H	8.080139	0.234871	-1.55332
77	C	-2.87889	-0.01062	-10.464
78	H	-3.15745	-1.00687	-10.8107
79	H	-3.67747	0.696334	-10.7063

80	H	-1.94985	0.292445	-10.9533
81	C	-10.8549	0.086424	0.001089
82	H	-11.2922	0.837028	-0.66328
83	H	-11.2769	-0.89261	-0.23061
84	H	-11.0745	0.334987	1.042624
85	C	-0.39221	-0.05857	7.980004
86	H	-0.62487	0.92125	8.399574
87	H	-1.05631	-0.80846	8.418759
88	H	0.649423	-0.3061	8.200454
89	Pt	-1.63283	-0.02133	-1.24228

Table S5 Coordinates of optimised ground state of D_2TMPyP4 in water

Tag	Symbol	X	Y	Z
1	N	-1.994727	0.558958	-0.052028
2	C	-3.122114	-0.263493	-0.094105
3	C	-2.485479	1.861694	-0.121141
4	C	-4.334265	0.540651	-0.231526
5	C	-3.941445	1.856758	-0.232536
6	H	-5.342459	0.168962	-0.330565
7	H	-4.583363	2.7218	-0.300328
8	N	0.605552	2.034114	-0.001966
9	C	1.914848	2.495219	0.040785
10	C	-0.284793	3.107404	0.05924
11	C	1.847233	3.934617	0.17336
12	C	0.517093	4.305377	0.165399
13	H	2.691665	4.597243	0.271872
14	H	0.134941	5.312384	0.224281
15	N	-0.616223	-2.039133	-0.096219
16	C	-1.924647	-2.488208	0.028555
17	C	0.272463	-3.10923	0.015297
18	C	-1.857438	-3.913735	0.262743
19	C	-0.528245	-4.288931	0.253266
20	H	-2.700849	-4.558761	0.450521
21	H	-0.144243	-5.280979	0.432023
22	N	1.984681	-0.559442	0.00306
23	C	2.469655	-1.856989	-0.145908
24	C	3.101857	0.26887	-0.122562
25	C	3.90356	-1.841083	-0.418065
26	C	4.295426	-0.524066	-0.403733
27	H	4.523301	-2.698594	-0.632288
28	H	5.284154	-0.140986	-0.605675
29	C	3.085741	1.694252	-0.026796
30	C	4.39378	2.398442	0.000224
31	C	4.705627	3.442225	-0.910884
32	C	5.391822	2.048434	0.945436
33	C	5.936224	4.084491	-0.85202
34	H	4.008243	3.73725	-1.685245
35	C	6.604403	2.729415	0.97813
36	H	5.218026	1.270479	1.678581
37	H	6.207217	4.873837	-1.541415
38	H	7.372325	2.50026	1.704761
39	C	1.682235	-3.047755	-0.056346
40	C	2.412914	-4.348468	-0.035977
41	C	2.139122	-5.365745	-0.983997
42	C	3.415655	-4.609904	0.928325
43	C	2.846521	-6.563506	-0.952171
44	H	1.400737	-5.222137	-1.763226
45	C	4.089743	-5.828969	0.92975
46	H	3.662781	-3.881879	1.691015
47	H	2.674695	-7.354955	-1.670108
48	H	4.851489	-6.063269	1.661259
49	C	-3.098227	-1.688602	-0.012638

50	C	-4.398456	-2.407014	0.049484
51	C	-4.71625	-3.44007	-0.868395
52	C	-5.375255	-2.089149	1.029469
53	C	-5.940423	-4.098332	-0.794745
54	H	-4.030402	-3.716968	-1.659721
55	C	-6.578124	-2.782746	1.074877
56	H	-5.190992	-1.326183	1.775642
57	H	-6.215225	-4.878824	-1.491924
58	H	-7.334801	-2.580368	1.821884
59	C	-1.690567	3.04271	-0.030299
60	C	-2.416164	4.353444	-0.030381
61	C	-3.101167	4.808286	-1.18149
62	C	-2.441223	5.175583	1.117885
63	C	-3.7651	6.031494	-1.160729
64	H	-3.106939	4.228249	-2.096225
65	C	-3.127021	6.390201	1.095353
66	H	-1.949446	4.874619	2.034907
67	H	-4.291714	6.418414	-2.023405
68	H	-3.174176	7.038868	1.959852
69	N	6.86865	3.735442	0.088354
70	N	-3.77413	6.804796	-0.032398
71	N	-6.853977	-3.77308	0.168866
72	N	3.807094	-6.785986	-0.004526
73	C	-4.507948	8.107739	-0.052584
74	H	-4.427984	8.580879	0.925875
75	H	-4.065827	8.757209	-0.811609
76	H	-5.559022	7.923532	-0.284646
77	C	8.167676	4.470437	0.132838
78	H	8.756079	4.110934	0.976872
79	H	8.716504	4.294389	-0.795391
80	H	7.97251	5.538697	0.252396
81	C	4.550973	-8.08216	-0.014184
82	H	5.052905	-8.199345	-0.977313
83	H	5.291782	-8.077745	0.78525
84	H	3.847614	-8.902824	0.143235
85	C	-8.160328	-4.490967	0.252551
86	H	-8.197731	-5.262196	-0.516964
87	H	-8.254084	-4.954073	1.237563
88	H	-8.974878	-3.779626	0.096889
89	H	0.34087	1.052761	-0.048856
90	H	-0.351498	-1.062472	-0.20033

Table S6 Coordinates of the optimised first singlet excited state of D_2TMPyP4 in water

Tag	Symbol	X	Y	Z
1	N	-1.994727	0.558958	-0.052028
2	C	-3.122114	-0.263493	-0.094105
3	C	-2.485479	1.861694	-0.121141
4	C	-4.334265	0.540651	-0.231526
5	C	-3.941445	1.856758	-0.232536
6	H	-5.342459	0.168962	-0.330565
7	H	-4.583363	2.7218	-0.300328
8	N	0.605552	2.034114	-0.001966
9	C	1.914848	2.495219	0.040785
10	C	-0.284793	3.107404	0.05924
11	C	1.847233	3.934617	0.17336
12	C	0.517093	4.305377	0.165399
13	H	2.691665	4.597243	0.271872
14	H	0.134941	5.312384	0.224281
15	N	-0.616223	-2.039133	-0.096219
16	C	-1.924647	-2.488208	0.028555
17	C	0.272463	-3.10923	0.015297
18	C	-1.857438	-3.913735	0.262743
19	C	-0.528245	-4.288931	0.253266
20	H	-2.700849	-4.558761	0.450521
21	H	-0.144243	-5.280979	0.432023
22	N	1.984681	-0.559442	0.00306
23	C	2.469655	-1.856989	-0.145908
24	C	3.101857	0.26887	-0.122562
25	C	3.90356	-1.841083	-0.418065
26	C	4.295426	-0.524066	-0.403733
27	H	4.523301	-2.698594	-0.632288
28	H	5.284154	-0.140986	-0.605675
29	C	3.085741	1.694252	-0.026796
30	C	4.39378	2.398442	0.000224
31	C	4.705627	3.442225	-0.910884
32	C	5.391822	2.048434	0.945436
33	C	5.936224	4.084491	-0.85202
34	H	4.008243	3.73725	-1.685245
35	C	6.604403	2.729415	0.97813
36	H	5.218026	1.270479	1.678581
37	H	6.207217	4.873837	-1.541415
38	H	7.372325	2.50026	1.704761
39	C	1.682235	-3.047755	-0.056346
40	C	2.412914	-4.348468	-0.035977
41	C	2.139122	-5.365745	-0.983997
42	C	3.415655	-4.609904	0.928325
43	C	2.846521	-6.563506	-0.952171
44	H	1.400737	-5.222137	-1.763226
45	C	4.089743	-5.828969	0.92975
46	H	3.662781	-3.881879	1.691015
47	H	2.674695	-7.354955	-1.670108
48	H	4.851489	-6.063269	1.661259
49	C	-3.098227	-1.688602	-0.012638

50	C	-4.398456	-2.407014	0.049484
51	C	-4.71625	-3.44007	-0.868395
52	C	-5.375255	-2.089149	1.029469
53	C	-5.940423	-4.098332	-0.794745
54	H	-4.030402	-3.716968	-1.659721
55	C	-6.578124	-2.782746	1.074877
56	H	-5.190992	-1.326183	1.775642
57	H	-6.215225	-4.878824	-1.491924
58	H	-7.334801	-2.580368	1.821884
59	C	-1.690567	3.04271	-0.030299
60	C	-2.416164	4.353444	-0.030381
61	C	-3.101167	4.808286	-1.18149
62	C	-2.441223	5.175583	1.117885
63	C	-3.7651	6.031494	-1.160729
64	H	-3.106939	4.228249	-2.096225
65	C	-3.127021	6.390201	1.095353
66	H	-1.949446	4.874619	2.034907
67	H	-4.291714	6.418414	-2.023405
68	H	-3.174176	7.038868	1.959852
69	N	6.86865	3.735442	0.088354
70	N	-3.77413	6.804796	-0.032398
71	N	-6.853977	-3.77308	0.168866
72	N	3.807094	-6.785986	-0.004526
73	C	-4.507948	8.107739	-0.052584
74	H	-4.427984	8.580879	0.925875
75	H	-4.065827	8.757209	-0.811609
76	H	-5.559022	7.923532	-0.284646
77	C	8.167676	4.470437	0.132838
78	H	8.756079	4.110934	0.976872
79	H	8.716504	4.294389	-0.795391
80	H	7.97251	5.538697	0.252396
81	C	4.550973	-8.08216	-0.014184
82	H	5.052905	-8.199345	-0.977313
83	H	5.291782	-8.077745	0.78525
84	H	3.847614	-8.902824	0.143235
85	C	-8.160328	-4.490967	0.252551
86	H	-8.197731	-5.262196	-0.516964
87	H	-8.254084	-4.954073	1.237563
88	H	-8.974878	-3.779626	0.096889
89	D	0.34087	1.052761	-0.048856
90	D	-0.351498	-1.062472	-0.20033

Table S7 TRIR kinetic fits – TMPyP4 + GMP/{d(GC)$_5$}$_2$

	τ (ns) monoexp. fit after 50 ps
TMPyP4-GMP (1636 cm^{-1})	0.61 ± 0.04
TMPyP4-GMP (1646 cm^{-1})	0.71 ± 0.11
TMPyP4-{d(GC)$_5$}$_2$ (1636 cm^{-1})	2.7 ± 0.4
TMPyP4-{d(GC)$_5$}$_2$ (1646 cm^{-1})	2.4 ± 0.6
TMPyP4-cMYC (1631 cm^{-1})	1.9 ± 0.3

Table S8 Biexponential fits to ps-TA data TMPyP4-GMP

system	**Wavelength (nm)**	**τ_1 (ps)**	**τ_2 (ps)**
TMPyP4- GMP	460 (transient)	51 ± 16 (12%)	540 ± 30 (88%)
TMPyP4- GMP	431 (bleach)	55 ± 9 (17%)	548 ± 23 (83%)

Experimental

Solution sample preparation

Solution samples for transient spectroscopy measurements were prepared in 50 mM phosphate buffered (pH 7) D_2O and a known volume of solution (25 –35 µL) was dropped between two CaF_2 (25 mm diameter, 2 mm thick) windows (Crystran Ltd, UK), separated by a Teflon spacer of 50 µm pathlength, in a demountable solution IR cell (Harrick Scientific Products Inc., New York).

Computational methods

All quantum chemical calculations were performed using Gaussian 16, Revision B.01[1]. The hybrid density function B3LYP was used in the majority of calculations.[2, 3] All calculations used the double zeta quality LanL2DZ basis set.[4-6] Structures were optimised to tight convergence criteria with the exception that the pyridinium methyl groups were frozen in the latter stages of the optimisations. The nature and energy of excited states were calculated using Time-Dependent Density Functional Theory methods (TD-DFT).[7-12] All calculations were corrected for water using the Polarizable Continuum Model (PCM).[13, 14] A scaling factor of 0.9803 was applied for all calculated wavenumbers to model the experimental spectra.

Cell culture

HeLa (human cervical cancer) cells were grown in Dulbecco's Modified Eagle Medium (DMEM) (Glutamax) supplemented with 10% fetal bovine serum and 50 µg/ml penicillin/streptomycin at 37 ˚C in a humidified atmosphere of 5% CO_2.

Confocal microscopy

Cells were seeded at a density of $1*10^5$ cells/dish in glass bottom wells and treated as indicated. Cells were viewed with a Leica confocal microscope and imaged with LAX software, 63X oil immersion lens. Compounds were excited by a 405 nm laser, emission 600-700 nm. Live cells were imaged directly, fixed cells were rinsed twice with PBS and incubated at -20 °C in methanol for 20 min, rinsed again and imaged in dH_2O.

Transient visible absorption measurement

Ps-TA measurements were performed on the ULTRA[15] apparatus at the Central Laser Facility (STFC Rutherford Appleton Laboratories, Harwell, UK). Part of the Ti:Sapphire laser output beam was used to generate a white light continuum (WLC) probe in a CaF_2 plate. The crystal plate was continuously rastered to avoid colour centre formation and to improve pulse-to-pulse stability in the probe. After the sample the WLC was dispersed through the grating monochromator and detected using a linear silicon array (Quantum Detectors). In front of the monochromator, a 400 nm notch filter was placed in order to remove scatter from the excitation beam. The polarisation of the pump pulses at the sample was at the magic angle relative to the probe, with an energy of 1 µJ and a spot size ca. 100-150 µm. The spectra were calibrated using a WCT-2065 metal oxide filter. The laser beam was mechanically chopped before the sample at 5 kHz with a C-995 chopper from Terahertz Technologies Inc. Samples were raster scanned in the x and y directions to minimise photodamage and re-excitation effects. Samples were checked before and after the experiment by UV/vis spectroscopy.

Time resolved infrared measurements of solution samples

The experiments were carried out in the Time Resolved Multiple Probe, TR^MPS, mode of the ULTRA instrument.[16] The mid IR probe was generated by difference frequency conversion of the signal and idler from an optical parametric amplifier pumped by 4 W of the output of a 10 kHz, 8W, 40 fs, 800 nm titanium sapphire laser and the pump by second harmonic of a 1 kHz, 4W, 120 fs, 800 nm titanium sapphire laser. The 373 nm pump beam (pulse length ca. 50 fs) was provided by the OPA (TOPAS, Light Conversion) pumped with the fundamental beam of the 10 kHz titanium sapphire laser. By operating in TR^MPS mode TRIR spectra spanning picosecond to microsecond timescales were produced. The

pump and probe beams were focused to approximately 150 and 100 μm diameter in the sample and set to the magic angle. TR^{M}PS data were acquired in sets of 10 probe pulses with the relative delay between pulses of the 1 and 10 kHz pulse trains controlled between 0 and 100 μs with sub-ps accuracy using optical and electrical delays. The multiple probing accesses delay times, t, t + 100 μs, t + 200 μs, etc. up to t + 900 μs, for each pump–probe delay, t, thus ten probe measurements are made for each pump pulse. The last probe pulse in the set of ten is used as a background and subtracted from the first nine to create the difference spectra presented.

Time resolved infrared measurements of cells

HeLa cells were seeded at a density of $6*10^5$ cells/well in 6 well plates containing sterilised CaF_2 discs and allowed to adhere overnight (or until nearly confluent). Cells were then rinsed and incubated in fresh phenol red-free FBS and antibiotic supplemented DMEM medium. Cells were treated with PtTMPyP4 (100 μM) for 4 h. Cells were then rinsed with phenol red-free medium and twice with phosphate-buffered saline, fixed for 20 min in methanol at -20°C, washed with dH_2O and allowed to air-dry. (Fixation of cells using formaldehyde was also attempted, however this was found to result in strong back-ground TRIR signals). Two fixed samples, separated by a 25 μm spacer, were then assembled into a in a demountable liquid cell and the TRIR spectra were recorded.

TRIR measurements using LIFEtime apparatus

TRIR measurements of the cells were carried out using the LIFEtime apparatus at the Central Laser Facility.[17] Briefly, a dual Pharos regenerative amplifier system (Light Conversion) was used to generate 1030 nm synchronised probe (100 kHz, 60 μJ, 180 fs) and pump (0.01-50 kHz, 150 μJ, 260 fs) pulses. The probe laser was used to drive two OPAs (Orpheus-ONE, Light Conversion), which generated tuneable mid-IR probe light via successive steps of optical parametric generation in BBO, KTA and difference frequency generation in GaSe. The two independently tuneable mid-IR probe beams were focussed through the sample with <70 μm spot sizes (FWHM) and dispersed onto two separate 128 pixel MCT array detectors (IR Associates). The second harmonic of the pump laser (515 nm) was used to pump a BBO-based OPA (Orpheus-HP, Light Conversion), generating 400 nm pump light from the second harmonic of the signal. The 400 nm pump light was delivered to the sample via a 1.2 m two-pass delay stage (Newport) and focussed through the sample with a spot size of 150 mm FWHM. Pump-probe delays were set using a combination of the delay stage (0-16 ns) and seeding of the two regenerative amplifiers with different seed pulses from their common oscillator (giving delays in 12.5 ns out to 10 ms). Delays beyond 10 μs could be achieved using the TR^{M}PS method,[16] which is based on lowering the repetition rate of the pump and measuring each probe pulse in the pump period separately. In the cell experiments, the samples were observed to recover on a μs timescale, and so 50 kHz pumping in combination with rastering of the sample was used. The 400 nm pump energy was 200 nJ – 500 nJ. Lower repetition rates were used in solution experiments.

References

1. M. J. Frisch, G. W. Trucks, H. B. Schlegel, G. E. Scuseria, M. A. Robb, J. R. Cheeseman, G. Scalmani, V. Barone, G. A. Petersson, H. Nakatsuji, X. Li, M. Caricato, A. V. Marenich, J. Bloino, B. G. Janesko, R. Gomperts, B. Mennucci, H. P. Hratchian, J. V. Ortiz, A. F. Izmaylov, J. L. Sonnenberg, D. Williams-Young, F. Ding, F. Lipparini, F. Egidi, J. Goings, B. Peng, A. Petrone, T. Henderson, D. Ranasinghe, V. G. Zakrzewski, J. Gao, N. Rega, G. Zheng, W. Liang, M. Hada, M. Ehara, K. Toyota, R. Fukuda, J. Hasegawa, M. Ishida, T. Nakajima, Y. Honda, O. Kitao, H. Nakai, T. Vreven, K. Throssell, J. A. Montgomery, J. E. Peralta, F. Ogliaro, M. J. Bearpark, J. J. Heyd, E. N. Brothers, K. N. Kudin, V. N. Staroverov, T. A. Keith, R. Kobayashi, J.

Normand, K. Raghavachari, A. P. Rendell, J. C. Burant, S. S. Iyengar, J. Tomasi, M. Cossi, J. M. Millam, M. Klene, C. Adamo, R. Cammi, J. W. Ochterski, R. L. Martin, K. Morokuma, O. Farkas, J. B. Foresman and D. J. Fox, *Gaussian 16*, Revision B.01, 2016, Gaussian, Inc., , Wallingford CT.

2. A. D. Becke, Density-Functional Thermochemistry 3. The Role of Exact Exchange, *J. Chem. Phys.*, 1993, **98**, 5648-5652.
3. C. T. Lee, W. T. Yang and R. G. Parr, Development of the Colle-Salvetti Correlation-Energy Formula into a Functional of the Electron-Density, *Phys. Rev. B*, 1988, **37**, 785-789.
4. T. H. Dunning Jr and P. J. Hay, in *Modern Theoretical Chemistry*, ed. H. F. Schaefer III, Plenum Press, New York, 1977, vol. 3, ch. 1-28.
5. P. J. Hay and W. R. Wadt, Ab Initio Effective Core Potentials for Molecular Calculations - Potentials for the Transition-Metal Atoms Sc to Hg, *J. Chem. Phys.*, 1985, **82**, 270-283.
6. P. J. Hay and W. R. Wadt, Ab Initio Effective Core Potentials for Molecular Calculations - Potentials for K to Au Including the Outermost Core Orbitals, *J. Chem. Phys.*, 1985, **82**, 299-310.
7. R. Bauernschmitt and R. Ahlrichs, Treatment of electronic excitations within the adiabatic approximation of time dependent density functional theory, *Chem. Phys. Lett.*, 1996, **256**, 454-464.
8. M. E. Casida, C. Jamorski, K. C. Casida and D. R. Salahub, Molecular excitation energies to high-lying bound states from time-dependent density-functional response theory: Characterization and correction of the time-dependent local density approximation ionization threshold, *J. Chem. Phys.*, 1998, **108**, 4439-4449.
9. R. E. Stratmann, G. E. Scuseria and M. J. Frisch, An efficient implementation of time-dependent density-functional theory for the calculation of excitation energies of large molecules, *J. Chem. Phys.*, 1998, **109**, 8218-8224.
10. C. Van Caillie and R. D. Amos, Geometric derivatives of excitation energies using SCF and DFT, *Chem. Phys. Lett.*, 1999, **308**, 249-255.
11. F. Furche and R. Ahlrichs, Adiabatic time-dependent density functional methods for excited state properties, *J. Chem. Phys.*, 2002, **117**, 7433-7447.
12. G. Scalmani, J. Frisch, B. Mennucci, J. Tomasi, R. Cammi and V. Barone, Geometries and properties of excited states in the gas phase and in solution: Theory and application of a time-dependent density functional theory polarizable continuum model, *J. Chem. Phys.*, 2006, **124**, 094107-094104.
13. M. Cossi, V. Barone, R. Cammi and J. Tomasi, Ab initio study of solvated molecules: A new implementation of the polarizable continuum mode, *Chem. Phys. Lett.*, 1996, **255**, 327-335.
14. J. Tomasi, B. Mennucci and R. Cammi, Quantum mechanical continuum solvation models, *Chem. Rev.*, 2005, **105**, 2999-3093.
15. G. M. Greetham, P. Burgos, Q. Cao, I. P. Clark, P. S. Codd, R. C. Farrow, M. W. George, M. Kogimtzis, P. Matousek, A. W. Parker, M. R. Pollard, D. A. Robinson, Z. J. Xin and M. Towrie, ULTRA: A unique instrument for time-resolved spectroscopy, *Appl. Spectrosc.*, 2010, **64**, 1311–1319.
16. G. M. Greetham, D. Sole, I. P. Clark, A. W. Parker, M. R. Pollard and M. Towrie, Time-resolved multiple probe spectroscopy, *Rev. Sci. Instrum.*, 2012, **83**, 103107.
17. G. M. Greetham, P. M. Donaldson, C. Nation, I. V. Sazanovich, I. P. Clark, D. J. Shaw, A. W. Parker and M. Towrie, A 100 kHz time-resolved multiple-probe femtosecond to second infrared absorption spectrometer, *Appl. Spectrosc.*, 2016, **70**, 645-653.